FACTA UNIVERSITATIS
Series: **Physics, Chemistry and Technology** Vol. 19, N° 2, 2021, pp. 69 - 79
https://doi.org/10.2298/FUPCT2102069N

Original scientific paper

ASSIGNMENT OF ^{1}H AND ^{13}C NMR SPECTRAL DATA OF DIASTEREOMERIC ACETALS DIRECTLY FROM THEIR MIXTURE BY SPECTRAL SIMULATION

UDC 543.429.23 : 547-316

Milan S. Nešić, Niko S. Radulović

Department of Chemistry, Faculty of Sciences and Mathematics, University of Niš,
Niš, Serbia

Abstract. *Herein, an NMR spectral analysis was performed of a mixture of diastereomeric acetals synthesized from 2-fluorobenzaldehyde and a racemic mixture of 4-methylpentan-2-ol. The simulated ^{1}H- and ^{13}C-NMR spectra of individual diastereomers, as well as their superimposed and summed spectra, were compared with the obtained experimental spectra. Spin simulation of proton signals was particularly useful for the assignment of the aromatic part of the molecules and of the diastereotopic protons of the methylene groups. The isomer NMR spectral data – chemical shifts, coupling constants, HMBC and NOESY interactions were systematized in appropriate tables and schemes.*

Key words: *NMR, spectra assignment, spin simulation, diastereomers, mixture*

1. INTRODUCTION

Non-stereospecific reactions of chiral compounds often lead to mixtures of diastereomers in which the share of each diastereomer cannot be easily determined. The separation of diastereomers, or isolation of a particular one, is often very long and demanding, and therefore the information on the contribution of target isomer(s) in the mixture deems very important, as to decide whether the separation should be tried at all. Encountering this problem is frequent, and to evade unnecessary laboratory work, solvents and potentially expensive stationary phases usage, a new approach was needed. In some cases, it is only the product ratio what is important for the confirmation of a reaction mechanism. The aim of this work was to illustrate an approach for the determination of

---

Received: December 9th, 2021; accepted: December 12th, 2021

Corresponding author: Niko S. Radulović, Department of Chemistry, Faculty of Sciences and Mathematics, University of Niš, Višegradska 33, 18000, Niš, Serbia, e-mail address: nikoradulovic@yahoo.com

composition of a mixture, in this particular case of diastereomeric acetals, and the assignment of NMR spectra of these diastereomers directly from their mixture.

Recently, we developed a diversity-oriented synthetic methodology for the preparation of acetals in good yield under very mild conditions, employing a PPh$_3$-CCl$_4$ reagent combination (Radulović and Nešić, 2016). This methodology, which utilizes stoichiometric amounts of an aldehyde and an alcohol was successfully applied to a wide scope of both carbonyls and alcohols. Among utilized alcohols there were chiral alcohols, i.e. racemic mixtures of these, which provided a mixture of diastereomeric acetals (Fig. 1).

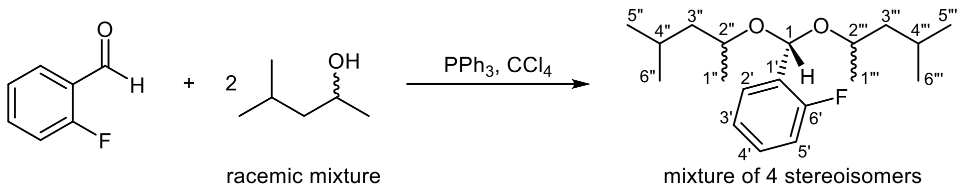

Fig. 1 PPh$_3$-CCl$_4$-mediated acetalization of 2-fluorobenzaldehyde and the racemic mixture of 4-methylpentan-2-ols

The relative ratio of the obtained diastereomers might shed light on the reaction mechanism; hence, it was important to be determined. The target acetal contains either two chiral centers, or one pseudochiral and two chiral centers, giving rise to 4 possible stereoisomeric products. The TIC chromatogram, obtained by GC-MS analysis of the reaction mixture, contained three peaks – two from *meso* diastereomers, and one from the enantiomeric pair. The relative ratio 52 : 29 : 19, obtained by TIC peak integration, suggested that the share of the enantiomeric pair is probably 52%, i.e. 26% of each enantiomer, while the *meso* compounds contribute with 29% and 19%.

2. MATERIALS AND METHODS

Chemicals. All herein used reagents (2-fluorobenzaldehyde, (±)-4-methylpentan-2-ol, PPh$_3$) and solvents (CCl$_4$, acetonitrile, pentane) were obtained from commercial sources (Sigma-Aldrich, St. Louis, MO, USA; Merck, Darmstadt, Germany; Carl Roth, Karlsruhe, Germany) and used as received, except that CCl$_4$ was additionally dried over molecular sieves.

Gas chromatography/mass spectrometry (GC-MS) analysis were performed on a Hewlett-Packard 6890N gas chromatograph equipped with a fused silica capillary column DB-5MS (5% polydiphenylsiloxane, 95% polydimethylsiloxane, 30 m × 0.25 mm, film thickness 0.25 μm; Agilent Technologies, Santa Clara, CA, USA) and coupled with a 5975B mass selective detector from the same company. The injector and interface were operated at 250 and 320 °C, respectively. The oven temperature was raised from 70 to 315 °C at a heating rate of 5 °C/min and then isothermally held for 30 min. As a carrier gas helium was used with flow 1.0 ml/min. The samples, 1 μl of the sample solutions in diethyl ether (10 mg dissolved in 1 ml), were injected in a split mode (split ratio 40:1). Mass selective detector was operated at the ionization energy of 70 eV, in the 35–850 amu range and scanning speed of 0.34 s. Relative abundance of the reaction mixture components was calculated from the peak-areas without the use of correction factors.

The ^{1}H and ^{13}C NMR spectra were recorded on a Bruker Avance III 400 MHz NMR spectrometer (Fällanden, Switzerland; ^{1}H at 400 MHz, ^{13}C at 100.6 MHz), equipped with a 5 mm dual ^{13}C/^{1}H probe head. All NMR spectra were recorded at 20 °C in deuterated chloroform with TMS as internal standard. Chemical shifts (δ) are reported in parts per million and referenced to TMS (δ_H = 0.00 ppm) in ^{1}H and to the (residual) solvent signal in ^{13}C NMR and heteronuclear 2D spectra (residual $CHCl_3$ δ_H = 7.26 ppm and $^{13}CDCl_3$ δ_C = 77.16 ppm). Scalar couplings are reported in Hertz (Hz). Sample (30 mg of the acetal mixture) was dissolved in 1 mL of deuterated chloroform, and 0.7 mL of the solution transferred into a 5 mm Wilmad, 528-TR-7 NMR tube.

Procedure for the acetal synthesis. A 10-ml round-bottom flask was charged with a solution of 2-fluorobenzaldehyde (124 mg, 1.0 mmol), (±)-4-methylpentan-2-ol (226 mg, 2.2 mmol), and triphenylphosphine (288 mg, 1.1 mmol) in dry CCl_4 (3 ml, 31.0 mmol). The reaction vessel was equipped with a $CaCl_2$-drying tube, and the reaction mixture was magnetically stirred for 7 days. After removing the excess CCl_4 on a rotary vacuum evaporator at 40 °C, the residue was taken up by pentane (2 x 5 ml). The dissolution was effectuated by exposing the contents of the flask to ultrasonic waves for 60 s, whereupon the pentane solution was transferred into a small separating funnel. Three consecutive partitions between pentane and MeCN (2 ml) were performed; MeCN layers were washed with a fresh amount (2 ml) of pentane; prior to the next partition, the two pentane layers were combined. The pentane layer, after the removal of the solvent, afforded 54 mg (17%) of the acetal mixture (>98% of stereomeric acetal, confirmed by GC-MS and ^{1}H and ^{13}C NMR spectroscopy).

3. RESULTS AND DISCUSSION

Enantiomers **1** and **2** (Fig. 2) have identical NMR spectra (R^1=S^2, R^2=S^1, Fig 2). The spatial arrangement of R^1 and S^2 alkoxy groups relative to the hydrogen and the aryl group at the acetal carbon is similar to that of R and S groups of **3** (blue and darker blue, Fig. 2). This means that the NMR signals of the nuclei pertaining to these groups will probably be similar, but not identical, due to the differing stereochemistry of the other alkoxy group, “on the other side” of the acetal carbon. The same is true for R^2 and S^1 compared to S and R groups of **4** (red and darker red). It follows that the part of the ^{1}H NMR spectrum corresponding to the alkoxy group signals should have 12 different doublets which originate from the methyl groups – 8 of them from the geminal (diastereotopic) ones and 4 which come from those next to the chiral center. The part of the observed spectrum which contains these signals is presented in Figure 3-F. Starting from the data extracted from the experimental ^{1}H NMR spectrum, spin simulations were performed in order to obtain the spectra of each of the isomers (A-C, Fig. 3). Spectrum D is a superposition of spectra A-C, while spectrum E (Fig. 3) represents their sum in a specific share as to match the observed spectrum F.

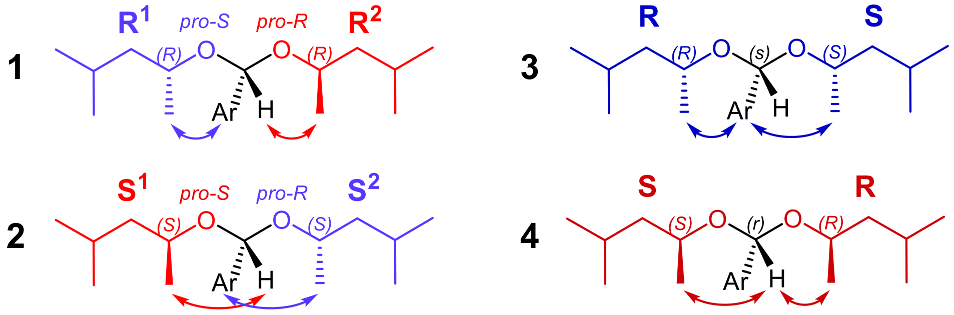

Fig. 2 The expected relationship of NMR signals of alkoxy groups from stereomeric acetals **1**-**4**

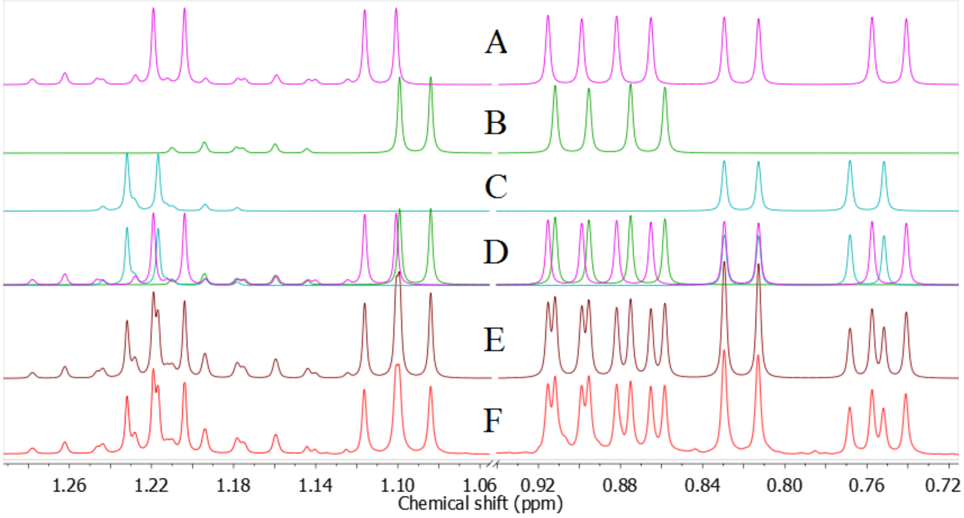

Fig. 3 Expansions of the experimental and simulated ^{1}H NMR spectra displaying signals originating from the methyl groups. A – the simulated spectrum of enantiomers **1** and **2**; B – the simulated spectrum of the more abundant *meso* compound; C – the simulated spectrum of the less abundant *meso* compound; D – the superposition of spectra A-C; E – the sum of spectra A-C in the relative share of 52:29:19; F – the experimental spectrum.

The signals which originate from the methine groups next to the geminal methyl groups (4 signals) and methylene groups (8 signals) are in the range from 1.10 to 1.85 ppm, while the signals of the carbinol proton are in the range from 3.60 to 3.90 ppm (4 signals). These overlapping signals can be seen in Figure 4-F and the left portion of Figure 3-F – partly overlapping with the mentioned signals of the methyl groups. Figure 4 presents the simulated (A-C), superimposed (D), summed (E) and experimental spectra (F) which contain the signals of the methylene and methine protons. Chemical shifts, coupling constants and other NMR data are presented in Tables 1-3 for each diastereomer.

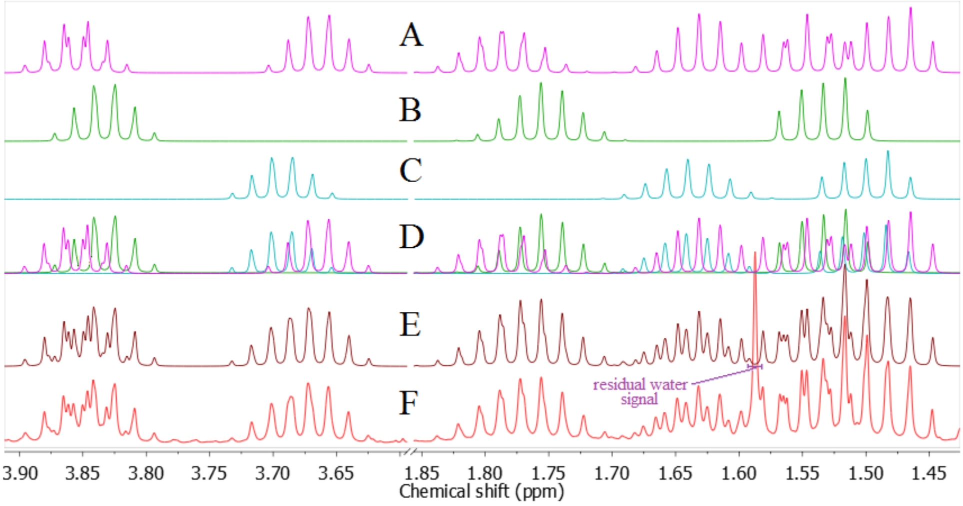

Fig. 4 Expansions of the experimental and simulated ^{1}H NMR spectra displaying signals originating from the methylene and methine protons. A – the simulated spectrum of enantiomers **1** and **2**; B – the simulated spectrum of the more abundant *meso* compound; C – the simulated spectrum of the less abundant *meso* compound; D – the superposition of spectra A-C; E – the sum of spectra A-C in the relative share of 52:29:19; F – the experimental spectrum.

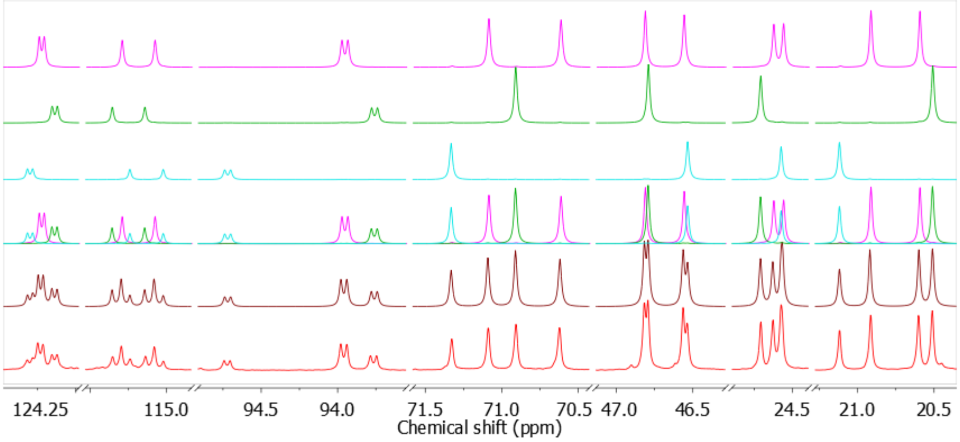

Fig. 5 Selected expansions of the experimental and simulated ^{13}C NMR spectra. A – the simulated spectrum of enantiomers **1** and **2**; B – the simulated spectrum of the more abundant *meso* compound; C – the simulated spectrum of the less abundant *meso* compound; D – the superposition of spectra A-C; E – the sum of spectra A-C in the relative share of 52:29:19; F – the experimental spectrum.

Assuming that carbons in analogous positions in different diastereomers have similar relaxation times, i.e. the intensities of their signals in the ^{13}C NMR spectra, an estimation of the stereoisomer content could be performed. The expansions of the simulated ^{13}C NMR spectra of the stereoisomers are presented in Figure 5, along with the experimental spectrum. The assigned ^{13}C NMR data can be found in Tables 1-3. Signals of the protons from the aromatic moieties, along with the one from the acetal carbon (Fig. 6), are shown on Figure 7. Three signals of the acetal protons and carbons are clearly visible (Fig. 7 and 5, respectively). The similarity of the signals coming from the aromatic moiety, complicated by hydrogen-fluorine coupling, made the assignment of these resonances difficult and was facilitated by the use of NMR data from a model compound (dihexyl acetal of 2-fluorobenzaldehyde) published previously (Radulović and Nešić, 2016). All of the mentioned led to the presented spin simulations (Fig. 7, A-C).

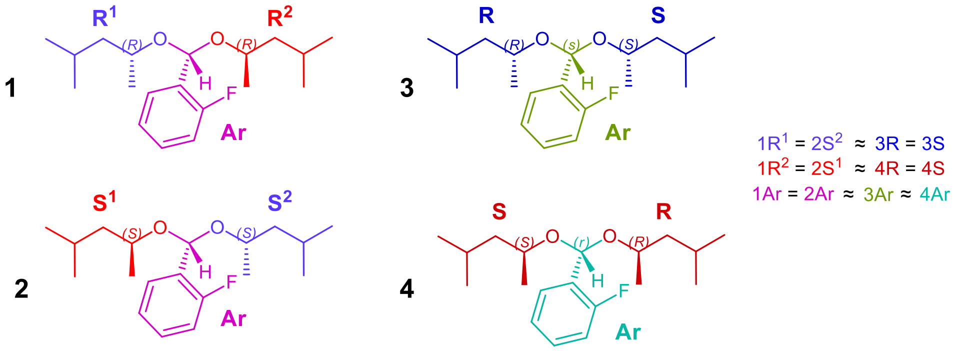

Fig. 6 The expected relationship of NMR signals of the aryl and acetal protons.

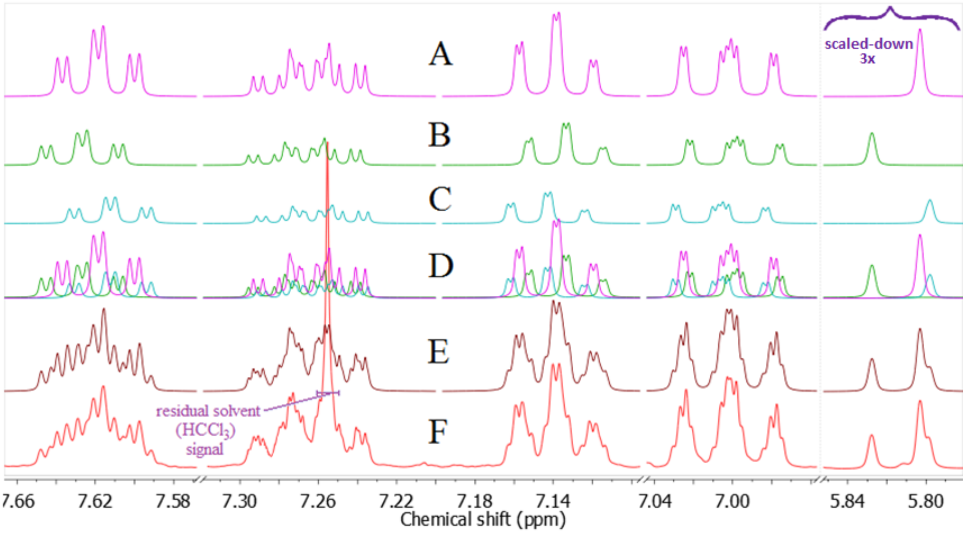

Fig. 7 Expansions of the experimental and simulated ^{1}H NMR spectra displaying signals originating from the aromatic moieties and the acetal hydrogen. A–F – as in Figure 5 legend.

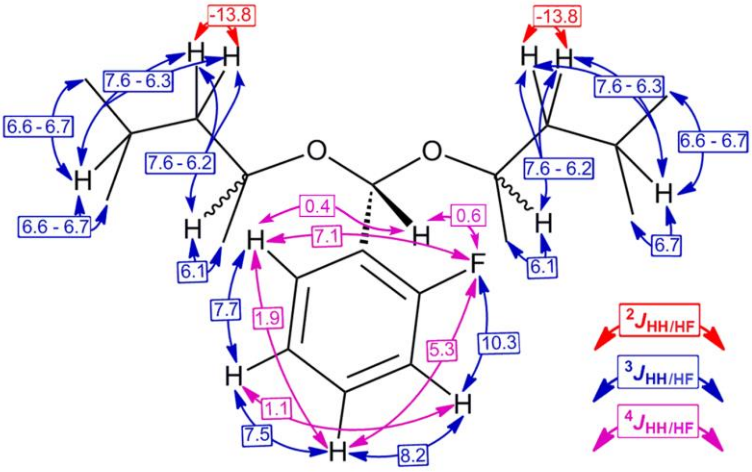

Fig. 8 Analysis of the observed ^{1}H-^{1}H coupling

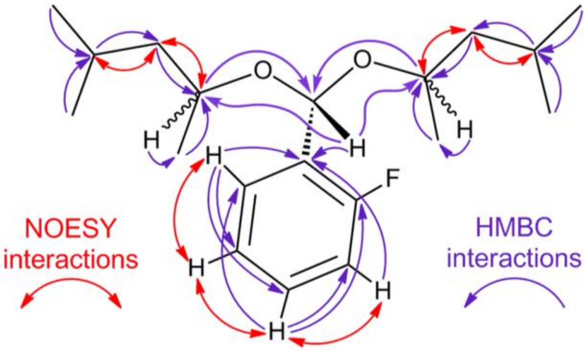

Fig. 9 Key observed HMBC and NOESY interactions

The assigned NMR chemical shifts of ^{1}H and ^{13}C signals and an interpretation of the couplings are given in Tables 1-3. All parameters used for the simulations are given, including the constants <0.4 Hz, which were disclosed in a series of selective homodecoupling experiments while higher in value vicinal, germinal, W and benzylic coupling constants are presented on Fig. 8. The range in values of coupling constants is given in cases when analogous coupling varied among the isomers. It is interesting to note that the values of ^{1}H-^{19}F W/*meta*-coupling constants were significantly higher than those of ^{1}H-^{1}H couplings. The HMBC and NOESY interactions are also summarized in these tables, and the key ones used during the assignment are presented on Fig. 9.

As stated earlier, the TIC chromatogram, obtained by GC-MS analysis of the reaction mixture, contained three peaks with the relative ratio of their areas 52 : 29 : 19, which suggested that the share of the enantiomeric pair was probably 52%, i.e. 26% of each enantiomer, while the *meso* compounds contributed with 29% and 19%. The approach presented above, the assignment of NMR spectral data directly from the mixture of compounds by spectral simulation, unequivocally confirmed these assumptions. This method turned out to be very successful even though the reaction mixture consisted of compounds with very similar NMR spectra, obtained in a similar yield.

Table 1 NMR spectral data of the chiral (*R**,*R**)-1-(bis((4-methylpentan-2-yl)oxy)methyl)-2-fluorobenzenes.

Position	δ_H (m, J (Hz), Integral)	δ_C (m, J (Hz), Integral)	HMBC[b]	NOESY[c]
1	5.8031 (dqtd, $^{4}J_{1,F} = 0.6$, $^{4}J_{1,6'} = {}^{4}J_{1,2''} = {}^{4}J_{1,2'''} = 0.4$, $^{5}J_{1,3'} = {}^{5}J_{1,5'} = 0.3$, $^{6}J_{1,4'} = 0.2$, 1 H)[a]	93.96 (d, $^{3}J_{1,F} = 3.9$, 1 C)	2’, 6’, 1”, 1’’’	/
1’	/	128.35 (d, $^{2}J_{1',F} = 13.7$, 1 C)	/	/
2’	/	160.28 (d, $^{1}J_{2',F} = 246.6$, 1 C)	/	/
3’	7.0024 (dddt, $^{3}J_{3',F} = 10.3$, $^{3}J_{3',4'} = 8.2$, $^{4}J_{3',5'} = 1.1$, $^{5}J_{1,3'} = {}^{5}J_{3',6'} = 0.3$, 1 H)	115.19 (d, $^{2}J_{3',F} = 21.7$, 1 C)	1’, 2’, 5’	4’
4’	7.2636 (ddddd, $^{3}J_{3',4'} = 8.2$, $^{3}J_{4',5'} = 7.5$, $^{4}J_{4',F} = 5.3$, $^{4}J_{4',6'} = 1.9$, $^{6}J_{1,4'} = 0.2$, 1 H)	129.85 (d, $^{3}J_{4',F} = 8.2$, 1 C)	2’, 3’, 6’	3’, 5’
5’	7.1393 (ddddd, $^{3}J_{5',6'} = 7.7$, $^{3}J_{4',5'} = 7.5$, $^{4}J_{3',5'} = 1.1$, $^{5}J_{5',F} = 0.4$, $^{5}J_{1,5'} = 0.3$, 1 H)	124.23 (d, $^{4}J_{5',F} = 3.4$, 1 C)	1’, 3’, 6’	4’, 6’
6’	7.6182 (ddddd, $^{3}J_{5',6'} = 7.7$, $^{4}J_{6',F} = 7.1$, $^{4}J_{4',6'} = 1.9$, $^{4}J_{1,6'} = 0.4$, $^{5}J_{3',6'} = 0.3$, 1 H)	128.62 (d, $^{3}J_{6',F} = 6.9$, 1 C)	1’, 2’, 4’	5’
1”	1.1085 (qt, $^{3}J_{1'',2''} = 6.1$, $^{4}J_{1'',3''a} = {}^{4}J_{1'',3''b} = 0.2$, 3 H)	20.92 (s, 1 C)	2”	2”
2”	3.8553 (ddqdd , $^{3}J_{2'',3''a} = 7.6$, $^{3}J_{2'',3''b} = 6.2$, $^{3}J_{1'',2''} = 6.1$, $^{4}J_{1,2''} = 0.4$, $^{4}J_{2'',4''} = 0.3$, 1 H)	71.09 (s, 1 C)	1”, 3”	1”, 3”
3”a	1.5457 (dddqqq, $^{2}J_{3''a'',3''b} = -13.8$, $^{3}J_{2'',3''a} = 7.6$, $^{3}J_{3''a,4''} = 6.3$, $^{4}J_{1'',3''a} = {}^{4}J_{3''a,5''} = {}^{4}J_{3''a,6''} = 0.2$, 1 H)	46.56 (s, 1 C)	2”, 4”	2”, 4”
3”b	1.1600 (dddqqq, $^{2}J_{3''a'',3''b} = -13.8$, $^{3}J_{3''b,4''} = 7.6$, $^{3}J_{2'',3''b} = 6.2$, $^{4}J_{1'',3''b} = {}^{4}J_{3''b,5''} = {}^{4}J_{3''b,6''} = 0.2$, 1 H)			
4”	1.7860 (dqqdd, $^{3}J_{3''b,4''} = 7.6$, $^{3}J_{4'',5''} = 6.7$, $^{3}J_{4'',6''} = 6.6$, $^{3}J_{3''a,4''} = 6.3$, $^{4}J_{2'',4''} = 0.3$, 1 H)	24.57 (s, 1 C)	3”, 5”, 6”	3”a, 3”b, 5”, 6”
5”	0.8736 (dt hex, $^{3}J_{4'',5''} = 6.7$, $^{4}J_{3''a,5''} = {}^{4}J_{3''b,5''} = {}^{4}J_{5'',6''} = 0.2$, 3 H)	22.87 (s, 1 C)	4”	4”
6”	0.9072 (dt hex, $^{3}J_{4'',6''} = 6.6$, $^{4}J_{3''a,6''} = {}^{4}J_{3''b,6''} = {}^{4}J_{5'',6''} = 0.2$, 3 H)	22.79 (s, 1 C)	4”	4”
1’’’	1.2115 (qt, $^{3}J_{1''',2'''} = 6.1$, $^{4}J_{1''',3'''a} = {}^{4}J_{1''',3'''b} = 0.2$, 3 H)	20.60 (s, 1 C)	2’’’	2’’’
2’’’	3.6640 (ddqdd , $^{3}J_{2''',3'''a} = 7.0$, $^{3}J_{2''',3'''b} = 6.3$, $^{3}J_{1''',2'''} = 6.1$, $^{4}J_{1,2'''} = 0.4$, $^{4}J_{2''',4'''} = 0.3$, 1 H)	70.62 (s 1 C)	1’’’, 3’’’	1’’’, 3’’’
3’’’a	1.4813 (dddqqq, $^{2}J_{3'''a'',3'''b} = -13.8$, $^{3}J_{3'''a,4'''} = 7.1$, $^{3}J_{2''',3'''a} = 7.0$, $^{4}J_{1''',3'''a} = {}^{4}J_{3'''a,5'''} = {}^{4}J_{3'''a,6'''} = 0.2$, 1 H)	46.82 (s, 1 C)	2’’’, 4’’’	2’’’, 4’’’
3’’’b	1.2465 (dtqqq, $^{2}J_{3'''a'',3'''b} = -13.8$, $^{3}J_{3'''b,4'''} = {}^{3}J_{2''',3'''b} = 6.3$, $^{4}J_{1''',3'''b} = {}^{4}J_{3'''b,5'''} = {}^{4}J_{3'''b,6'''} = 0.2$, 1 H)			
4’’’	1.6303 (dqqdd, $^{3}J_{3'''a,4'''} = 7.1$, $^{3}J_{4''',5'''} = {}^{3}J_{4''',6'''} = 6.7$, $^{3}J_{3'''b,4'''} = 6.3$, $^{4}J_{2''',4'''} = 0.3$, 1 H)	24.63 (s, 1 C)	3’’’, 5’’’, 6’’’	3’’’a, 3’’’b, 5’’’, 6’’’
5’’’	0.7492 (qddq, $^{3}J_{4''',5'''} = 6.7$, $^{4}J_{3'''a,5'''} = {}^{4}J_{3'''b,5'''} = {}^{4}J_{5''',6'''} = 0.2$, 3 H)	22.87 (s, 1 C)	4’’’	4’’’
6’’’	0.8212 (qddq, $^{3}J_{4''',6'''} = 6.7$, $^{4}J_{3'''a,6'''} = {}^{4}J_{3'''b,6'''} = {}^{4}J_{5''',6'''} = 0.2$, 3 H)	23.05 (s, 1 C)	4’’’	4’’’

[a] Coupling constant values were initially inferred from ^{1}H homoselective decoupling NMR experiments and afterward refined through a manual iterative full spin analysis. For details, cf. Experimental part. [b] gHMBC correlations observed between the hydrogen in this row and the carbon in the listed position. [c] Cross-peaks observed in the NOESY spectrum.

Table 2 NMR spectral data of the more abundant *meso* diastereomer of 1-(bis((4-methylpentan-2-yl)oxy)methyl)-2-fluorobenzene.

Position	δ_H (m, J (Hz), Integral)	δ_C (m, J (Hz), Integral)	HMBC[b]	NOESY[c]
1	5.8277 (dqtd, $^{4}J_{1,F} = 0.6$, $^{4}J_{1,6'} = {}^{4}J_{1,2''} = {}^{4}J_{1,2'''} = 0.4$, $^{5}J_{1,3'} = {}^{5}J_{1,5'} = 0.3$, $^{6}J_{1,4'} = 0.2$, 1 H)[a]	93.76 (d, $^{3}J_{1,F} = 4.0$, 1 C)	2’, 6’, 1”, 1”’	/
1’	/	128.09 (d, $^{2}J_{1',F} = 13.2$, 1 C)	/	/
2’	/	160.06 (d, $^{1}J_{2',F} = 246.8$, 1 C)	/	/
3’	6.9992 (dddt, $^{3}J_{3',F} = 10.3$, $^{3}J_{3',4'} = 8.2$, $^{4}J_{3',5'} = 1.1$, $^{5}J_{1,3'} = {}^{5}J_{3',6'} = 0.3$, 1 H)	115.25 (d, $^{2}J_{3',F} = 21.6$, 1 C)	1’, 2’, 5’	4’
4’	7.2660 (ddddd, $^{3}J_{3',4'} = 8.2$, $^{3}J_{4',5'} = 7.5$, $^{4}J_{4',F} = 5.3$, $^{4}J_{4',6'} = 1.9$, $^{6}J_{1,4'} = 0.2$, 1 H)	129.87 (d, $^{3}J_{4',F} = 8.1$, 1 C)	2’, 3’, 6’	3’, 5’
5’	7.1343 (ddddd, $^{3}J_{5',6'} = 7.7$, $^{3}J_{4',5'} = 7.5$, $^{4}J_{3',5'} = 1.1$, $^{5}J_{5',F} = 0.4$, $^{5}J_{1,5'} = 0.3$, 1 H)	124.14 (d, $^{4}J_{5',F} = 3.4$, 1 C)	1’, 3’, 6’	4’, 6’
6’	7.6265 (ddddd, $^{3}J_{5',6'} = 7.7$, $^{4}J_{6',F} = 7.1$, $^{3}J_{4',6'} = 1.9$, $^{4}J_{1,6'} = 0.4$, $^{5}J_{3',6'} = 0.3$, 1 H)	128.50 (d, $^{3}J_{6',F} = 5.0$, 1 C)	1’, 2’, 4’	5’
1”/1”’	1.0916 (qt, $^{3}J_{1'',2''} = 6.1$, $^{4}J_{1'',3''a} = {}^{4}J_{1'',3''b} = 0.2$, 6 H)	20.51 (s, 2 C)	2”	2”
2”/2”’	3.8328 (ddqdd , $^{3}J_{2'',3''a} = 7.0$, $^{3}J_{2'',3''b} = 6.2$, $^{3}J_{1'',2''} = 6.1$, $^{4}J_{1,2''} = 0.4$, $^{4}J_{2'',4''} = 0.3$, 2 H)	70.91 (s, 2 C)	1”, 3”	1”, 3”
3”a/3”’a	1.5331 (dddqqq, $^{2}J_{3''a'',3''b} = -13.8$, $^{3}J_{3''a,4''} = 7.1$, $^{3}J_{2'',3''a} = 7.0$, $^{4}J_{1'',3''a} = {}^{4}J_{3''a,5''} = {}^{4}J_{3''a,6''} = 0.2$, 2 H)	46.79 (s, 2 C)	2”, 4”	2”, 4”
3”b/3”’b	1.1780 (dddqqq, $^{2}J_{3''a'',3''b} = -13.8$, $^{3}J_{3''b,4''} = 6.3$, $^{3}J_{2'',3''b} = 6.2$, $^{4}J_{1'',3''b} = {}^{4}J_{3''b,5''} = {}^{4}J_{3''b,6''} = 0.2$, 2 H)			
4”/4”’	1.7552 (dqqdd, $^{3}J_{3''a,4''} = 7.1$, $^{3}J_{4'',5''} = 6.7$, $^{3}J_{4'',6''} = 6.6$, $^{3}J_{3''b,4''} = 6.3$, $^{4}J_{2'',4''} = 0.3$, 2 H)	24.71 (s, 2 C)	3”, 5”, 6”	3”a, 3”b, 5”, 6”
5”/5”’	0.8668 (dddq, $^{3}J_{4'',5''} = 6.7$, $^{4}J_{3''a,5''} = {}^{4}J_{3''b,5''} = {}^{4}J_{5'',6''} = 0.2$, 6 H)	22.92 (s, 2 C)	4”	4”
6”/6”’	0.9037 (dddq, $^{3}J_{4'',6''} = 6.6$, $^{4}J_{3''a,6''} = {}^{4}J_{3''b,6''} = {}^{4}J_{5'',6''} = 0.2$, 6 H)	23.05 (s, 2 C)	4”	4”

[a] Coupling constant values were initially inferred from ^{1}H homoselective decoupling NMR experiments and afterward refined through a manual iterative full spin analysis. For details, cf. Experimental part. [b] gHMBC correlations observed between the hydrogen in this row and the carbon in the listed position. [c] Cross-peaks observed in the NOESY spectrum.

Table 3 NMR spectral data of the less abundant *meso* diastereomer of 1-(bis((4-methylpentan-2-yl)oxy)methyl)-2-fluorobenzene.

Position	δ_H (m, J (Hz), Integral)	δ_C (m, J (Hz), Integral)	HMBC[b]	NOESY[c]
1	5.7982 (dqtd, $^{4}J_{1,\mathrm{F}} = 0.6$, $^{4}J_{1,6'} = {}^{4}J_{1,2''} = {}^{4}J_{1,2'''} = 0.4$, $^{5}J_{1,3'} = {}^{5}J_{1,5'} = 0.3$, $^{6}J_{1,4'} = 0.2$, 1 H)[a]	94.72 (d, $^{3}J_{1,\mathrm{F}} = 3.9$, 1 C)	2’, 6’, 1”, 1”’	/
1’	/	128.51 (d, $^{2}J_{1'/,\mathrm{F}} = 13.6$, 1 C)	/	/
2’	/	160.42 (d, $^{1}J_{2',\mathrm{F}} = 246.5$, 1 C)	/	/
3’	7.0065 (dddt, $^{3}J_{3',\mathrm{F}} = 10.3$, $^{3}J_{3',4'} = 8.2$, $^{4}J_{3',5'} = 1.1$, $^{5}J_{1,3'} = {}^{5}J_{3',6'} = 0.3$, 1 H)	115.13 (d, $^{2}J_{3',\mathrm{F}} = 21.9$, 1 C)	1’, 2’, 5’	4’
4’	7.2620 (ddddd, $^{3}J_{3',4'} = 8.2$, $^{3}J_{4',5'} = 7.5$, $^{4}J_{4',\mathrm{F}} = 5.2$, $^{4}J_{4',6'} = 1.9$, $^{6}J_{1,4'} = 0.2$, 1 H)	129.80 (d, $^{3}J_{4',\mathrm{F}} = 8.2$, 1 C)	2’, 3’, 6’	3’, 5’
5’	7.1437 (ddddd, $^{3}J_{5',6'} = 7.7$, $^{3}J_{4',5'} = 7.5$, $^{4}J_{3',5'} = 1.1$, $^{5}J_{5',\mathrm{F}} = 0.4$, $^{5}J_{1,5'} = 0.3$, 1 H)	124.30 (d, $^{4}J_{5',\mathrm{F}} = 3.5$, 1 C)	1’, 3’, 6’	4’, 6’
6’	7.6121 (ddddd, $^{3}J_{5',6'} = 7.7$, $^{4}J_{6',\mathrm{F}} = 7.1$, $^{3}J_{4',6'} = 1.9$, $^{4}J_{1,6'} = 0.4$, $^{5}J_{3',6'} = 0.3$, 1 H)	128.50 (d, $^{3}J_{6',\mathrm{F}} = 5.0$, 1 C)	1’, 2’, 4’	5’
1”/1”’	1.2243 (qt, $^{3}J_{1'',2''} = 6.05$, $^{4}J_{1'',3''a} = {}^{4}J_{1'',3''b} = 0.2$, 6 H)	21.12 (s, 2 C)	2”	2”
2”/2”’	3.6932 (ddqdd , $^{3}J_{2'',3''a} = 7.0$, $^{3}J_{2'',3''b} = 6.3$, $^{3}J_{1'',2''} = 6.05$, $^{4}J_{1,2''} = 0.4$, $^{4}J_{2'',4''} = 0.3$, 2 H)	71.33 (s, 2 C)	1”, 3”	1”, 3”
3”a/3”’a	1.5009 (dddqqq, $^{2}J_{3''a'',3''b} = -13.8$, $^{3}J_{3''a,4''} = 7.2$, $^{3}J_{2'',3''a} = 7.0$, $^{4}J_{1'',3''a} = {}^{4}J_{3''a,5''} = {}^{4}J_{3''a,6''} = 0.2$, 2 H)	46.54 (s, 2 C)	2”, 4”	2”, 4”
3”b/3”’b	1.2122 (dddqqq, $^{2}J_{3''a'',3''b} = -13.8$, $^{3}J_{2'',3''b} = 6.3$, $^{3}J_{3''b,4''} = 6.2$, $^{4}J_{1'',3''b} = {}^{4}J_{3''b,5''} = {}^{4}J_{3''b,6''} = 0.2$, 2 H)			
4”/4”’	1.6405 (dqqdd, $^{3}J_{3''a,4''} = 7.2$, $^{3}J_{4'',6''} = 6.7$, $^{3}J_{4'',5''} = 6.65$, $^{3}J_{3''b,4''} = 6.2$, $^{4}J_{2'',4''} = 0.3$, 2 H)	24.57 (s, 2 C)	3”, 5”, 6”	3”a, 3”b, 5”, 6”
5”/5”’	0.7600 (dddq, $^{3}J_{4'',5''} = 6.65$, $^{4}J_{3''a,5''} = {}^{4}J_{3''b,5''} = {}^{4}J_{5'',6''} = 0.2$, 6 H)	22.92 (s, 2 C)	4”	4”
6”/6”’	0.8212 (dddq, $^{3}J_{4'',6''} = 6.7$, $^{4}J_{3''a,6''} = {}^{4}J_{3''b,6''} = {}^{4}J_{5'',6''} = 0.2$, 6 H)	22.83 (s, 2 C)	4”	4”

[a] Coupling constant values were initially inferred from ^{1}H homoselective decoupling NMR experiments and afterward refined through a manual iterative full spin analysis. For details, cf. Experimental part. [b] gHMBC correlations observed between the hydrogen in this row and the carbon in the listed position. [c] Cross-peaks observed in the NOESY spectrum.

Acknowledgement: *The paper is a part of the Ph.D. thesis of Milan Nešić supervised by Niko Radulović. The authors would like to thank to the Ministry of Education, Science and Technological Development of the Republic of Serbia [Project No. 172061, No. contract 451-03-9/2021-14/200124] for the financial support of this work.*

REFERENCES

Radulović N., Nešić M., 2016. RSC Adv., 6, 93068–93080. doi:10.1039/C6RA19980A

ASIGNACIJA ^{1}H I ^{13}C NMR SPEKTRALNIH PODATAKA DIJASTEREOMERNIH ACETALA SPEKTRALNOM SIMULACIJOM DIREKTNO IZ NJIHOVE SMEŠE

U ovom radu izvršena je NMR spektralna analiza smeše dijastereomernih acetala sintetisanih iz 2-fluorbenzaldehida i racemske smeše 4-metilpentan-2-ola. Simulirani ^{1}*H- i* ^{13}*C-NMR spektri pojedinačnih dijastereomera, kao i njihovi preklopljeni i sumirani spektri su upoređeni sa eksperimentalnim spektrima. Spinska simulacija signala vodonika bila je posebno korisna za asignaciju aromatičnog dela molekula i dijastereotopnih protona metilenskih grupa. NMR-spektralni podaci izomera – hemijska pomeranja, konstante kuplovanja, HMBC i NOESY interakcije sistematizovani su u odgovarajućim tabelama i šemama.*

Ključne reči: *NMR, asignacija spektara, spinska simulacija, dijastereomeri, smeša*